

# In-Grain Misorientation Axes Distribution of rolled AZ31 and Its Correlation with Deformation Mechanism



Young B. Chun and Chris H. J. Davies

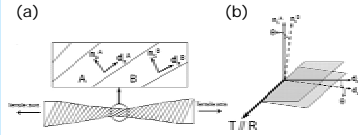
Department of Materials Engineering, Monash University, VIC 3800, Australia

## Introduction

Mg alloys promise considerable weight savings of automotive and aerospace industries, due to their low density and high specific strength. However, they have a limited formability at room temperature due to an insufficient number of slip modes, which in turn limits the wide application of wrought Mg alloys. For alloy/process design strategies to improve the formability of Mg alloys, it is necessary to understand deformation mechanism, i.e., slip or twinning, that govern the plasticity of Mg alloys. Earlier works on deformation mechanism of Mg alloys have relied mainly on surface trace analysis and/or TEM-based Burgers vector determination. These approaches, however, may introduce great uncertainty in drawing general conclusions on deformation modes responsible for plasticity of bulk polycrystals since the number of grains accessible is quite limited. In the present work, we have developed a new approach, which is based on analysis of in-grain misorientation axes (IGMA) and allows identifying active slip mode for quite large number of grains. Using this approach, we have made attempt to uncover the active slip mode of individual grains in cold-rolled AZ31 with particular attention being focused on orientation-dependency of active slip mode.

## Approach – IGMA Analysis

In order to study deformation mechanism of AZ31, we employed a new approach, termed '**IGMA analysis**'. Determination of active slip mode by this approach is based on the following assumptions [1,2]: (i) deformation by slip causes a bending of crystal lattice as shown in Figure 1(a), (ii) this bending takes about an axis (called '**Taylor axis**') and gives rise to a rotation of all crystallographic planes about this axis and (iii) the Taylor axis is usually at a crystallographic direction of low indices lying in the slip plane and perpendicular to the slip direction, and thus can be defined as  $T_s = n_s \times d_s$  ( $T_s$ ,  $n_s$  and  $d_s$  are the Taylor axis, slip plane normal and slip direction, respectively, of slip mode,  $s$ ), as shown in Figure 1(b). Based on this assumptions, it is possible to determine the dominant slip mode in a given deformed grain by finding matching Taylor axis to the experimentally-measured in-grain misorientation axis. Slip modes and the corresponding Taylor axes available in Mg are summarized in Table 1.



Slip modes	Total number of slip variants	Taylor axis	Total number of variants of the Taylor axis
$\{001\} \langle 110 \rangle$	3	$\langle 0001 \rangle$	1
$\{0002\} \langle 110 \rangle$	3	$\langle 0110 \rangle$	3
$\{01\bar{1}2\} \langle 11\bar{2} \rangle$	6	$\langle 1100 \rangle$	3

Figure 1. Schematics illustrating the main assumptions of IGMA analysis: (a) lattice bending under action of slip and (b) lattice rotation about the Taylor axis.

Table 1. Summary of slip modes available in Mg and the corresponding Taylor axis.

## Experimental Procedures

Commercial AZ31 plates with four different starting textures (schematically shown in Figure 2) were cold-rolled to 10% reduction in thickness. The transverse cross sections cut from the rolled plates were mechanically ground and then electro-polished for EBSD measurement. Distributions of IGMA for individual deformed grains were obtained from EBSD measurement by the following procedures: (i) selecting a grain of interest, (ii) determining the misorientation axes for all possible neighboring lattice-point pairs belonging to the selected grain, and (iii) plotting the distribution intensities of misorientation axes (with misorientations between 0.5° and 1.5°) on standard unit triangle. Step size used for the EBSD scan was 0.5 μm.

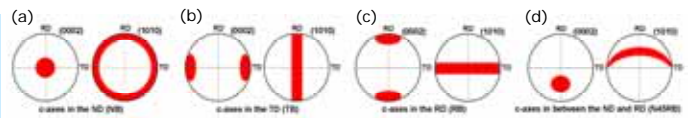


Figure 2. Schematic representations of the basal and prism pole figures showing four different starting textures of AZ31 plates used in the present work: (a) NB, (b) TB, (c) RB, and (d) N45RB.

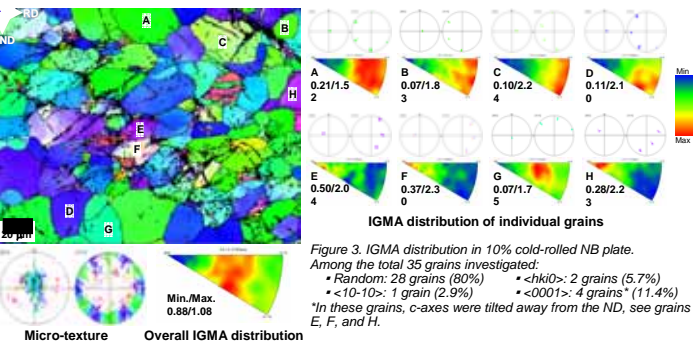


Figure 3. IGMA distribution in 10% cold-rolled NB plate. Among the total 35 grains investigated:  
 • Random: 28 grains (80%) •  $\langle hki0 \rangle$ : 2 grains (5.7%)  
 •  $\langle 10\text{-}10 \rangle$ : 1 grain (2.9%) •  $\langle 0001 \rangle$ : 4 grains\* (11.4%)  
 \*In these grains, c-axes were tilted away from the ND, see grains E, F, and H.

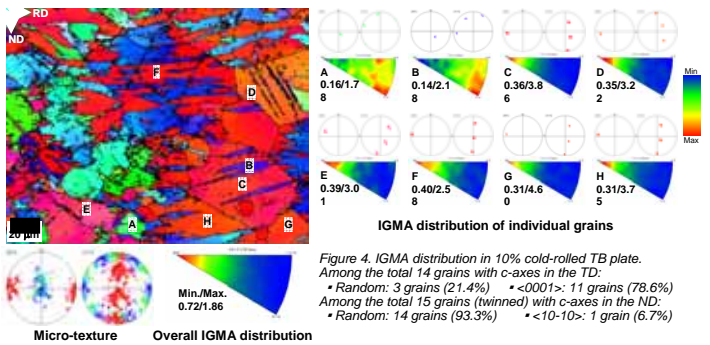


Figure 4. IGMA distribution in 10% cold-rolled TB plate. Among the total 14 grains with c-axes in the TD:  
 • Random: 3 grains (21.4%) •  $\langle 0001 \rangle$ : 11 grains (78.6%)  
 Among the total 15 grains (twinned) with c-axes in the ND:  
 • Random: 14 grains (93.3%) •  $\langle 10\text{-}10 \rangle$ : 1 grain (6.7%)

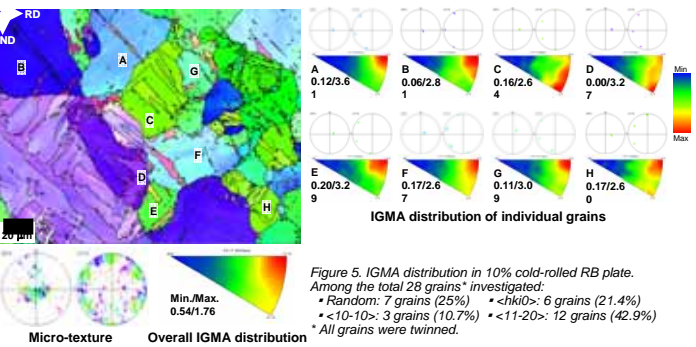


Figure 5. IGMA distribution in 10% cold-rolled RB plate. Among the total 28 grains\* investigated:  
 • Random: 7 grains (25%) •  $\langle hki0 \rangle$ : 6 grains (21.4%)  
 •  $\langle 10\text{-}10 \rangle$ : 3 grains (10.7%) •  $\langle 11\text{-}20 \rangle$ : 12 grains (42.9%)  
 \*All grains were twinned.

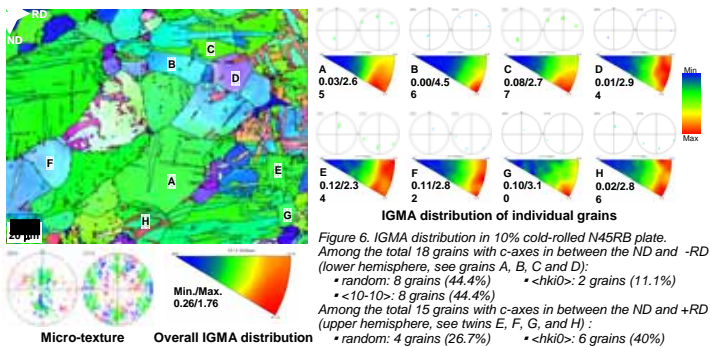


Figure 6. IGMA distribution in 10% cold-rolled N45RB plate. Among the total 18 grains with c-axes in between the ND and -RD (lower hemisphere, see grains A, B, C and D):  
 • Random: 8 grains (44.4%) •  $\langle hki0 \rangle$ : 2 grains (11.1%)  
 •  $\langle 10\text{-}10 \rangle$ : 8 grains (44.4%)  
 Among the total 15 grains with c-axes in between the ND and +RD (upper hemisphere, see twins E, F, G, and H):  
 • Random: 4 grains (26.7%) •  $\langle hki0 \rangle$ : 6 grains (40%)  
 •  $\langle 10\text{-}10 \rangle$ : 5 grain (33.3%)

## Results and Discussion

The IGMA analyses for 10% cold-rolled AZ31 plates revealed that the deformed individual grains exhibit characteristic IGMA distributions, depending on their crystallographic orientations, as shown in Figures 3-6. By considering the Taylor axis (Table 1) and the Schmid factor distribution (Figure 7) of slip modes available in Mg, the active slip mode in each orientation group is determined as follows:

- NB orientations:** Most of grains belonging to these orientations showed random distribution (distribution with maximum intensity value of less than 2 m.u.d. is considered as random) of IGMA. This implies that there was no specific slip mode that prevailed over other slip modes and thus that the externally imposed strain was accommodated by co-activation of various slip modes.
- TB orientations:** These grains exhibited a characteristics distribution pattern in which the IGMA are concentrated towards  $\langle 0001 \rangle$ . This distribution is indicative of **dominant activation of prism  $\langle a \rangle$  slip**, since the  $\langle 0001 \rangle$  is the Taylor axis of the latter slip mode. This rationale is also supported by their high Schmid factors at those orientations (Figure 7(a)).
- RB orientations:** In these grains, the IGMA were preferentially distributed around either  $\langle 10\text{-}10 \rangle$ ,  $\langle 11\text{-}20 \rangle$  or  $\langle hki0 \rangle$ . Since these IGMA distributions are expected when favorable slip variants of  $\{1122\} \langle 1123 \rangle$  slip are co-activated and also because the Schmid factor of the latter slip mode is obviously higher than those of any other slip modes at these orientations (Figure 7(c)),  $\{1122\} \langle 1123 \rangle$  slip can be considered as an active slip mode in these grains.
- N45RB orientations:** As expected from its low critical resolved shear stress and the high Schmid factor at these orientations, basal  $\langle a \rangle$  slip did dominate in these grains and, in turn, resulted in two characteristic IGMA distributions, one with the peak intensity around  $\langle 10\text{-}10 \rangle$  and the other around  $\langle hki0 \rangle$ . The former distribution is expected when only one variant of basal  $\langle a \rangle$  slip is activated while the latter distribution can be caused by duplex slip in two different  $\langle a \rangle$  directions on basal plane.

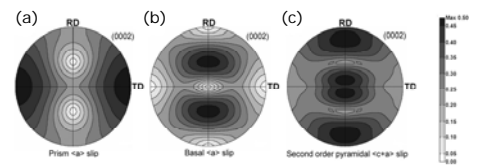


Figure 7. Schmid factor distributions of the selected slip systems available in Mg under plane-strain compression: (a) prism  $\langle a \rangle$  slip, (b) basal  $\langle a \rangle$  slip and (c)  $\{1122\} \langle 1123 \rangle$  slip.

## Acknowledgement

This work was supported by Australian Research Council. The present authors are grateful to Dr. M.J. Bataini for providing the Schmid factor distributions.

## References

- [1] E.J. Rappoport, C.S. Hartley, Trans AIME, 218 (1960) 869.
- [2] P. Bastien, P. Pointu, J Nucl Mater, 5 (1962) 101.

## Summary

From the analysis of in-grain misorientation axes distribution in the 10% cold-rolled AZ31 plates, it was confirmed that the IGMA distribution of a deformed is quite dependent on their crystallographic orientations, indicating orientation dependence of active slip mode. By using this technique, basal  $\langle a \rangle$  slip,  $\{1122\} \langle 1123 \rangle$  slip and prism  $\langle a \rangle$  slip were determined as an active slip mode at three different orientations groups, the N45RB, RB and TB, respectively.